LIGHTCURVES OF TWELVE ASTEROIDS

Eric V. Dose
3167 San Mateo Blvd NE #329
Albuquerque, NM 87110
mp@ericdose.com

(Received: 2023 January 14)

We present lightcurves, synodic rotation periods, and G value (H-G) estimates for twelve asteroids.

We present asteroid lightcurves obtained via the workflow process described by Dose (2020) and as later improved (Dose, 2021). This workflow applies to each image an ensemble of typically 15-60 nearby comparison ("comp") stars selected from the ATLAS refcat2 catalog (Tonry et al., 2018). Custom diagnostic plots and the abundance of comp stars allow for rapid identification and removal of outlier, variable, and poorly measured comp stars.

The product of this custom workflow is one night's time series of absolute magnitudes for the target asteroid, all on Sloan r' (SR) catalog basis. These magnitudes are corrected for instrument transforms, sky extinction, and image-to-image ("cirrus") fluctuations and thus represent magnitudes at the top of earth's atmosphere. These magnitudes are imported directly into *MPO Canopus* software (Warner, 2021) where they are adjusted for distances and phase-angle dependence, fit by Fourier analysis including identifying and ruling out of aliases, and plotted.

Phase-angle dependence is corrected with a H-G model, using the G value minimizing best-fit RMS error across all nights' data; in rare cases for which we cannot estimate an asteroid's G value, we apply the Minor Planet Center's nominal value of 0.15. No nightly zero-point adjustments (Delta Comps in *MPO Canopus* terminology) were made to any session herein, other than by estimating G, which practice we note introduces only one new fitting term vs many more terms (number of nights - 1) when applying non-zero Delta Comps.

Lightcurve Results

Twelve asteroids were observed from New Mexico Skies observatory at 2310 meters elevation in southern New Mexico. Images were acquired with a 0.35-meter SCT reduced to f/7.7; a SBIG STXL-6303E camera cooled to -35 C and fitted with an Exoplanet/Blue Blocker (BB) filter (Astrodon); and a PlaneWave L-500 mount. The equipment was operated remotely via ACP software (DC-3 Dreams, version 8.3), running plan files generated for each night by the author's python scripts (Dose, 2020). Exposures were autoguided, and exposure times targeted 3-5 millimagnitudes uncertainty in asteroid instrumental magnitude, subject to a minimum exposure of 150 seconds to ensure suitable comp-star photometry, and to a maximum of 900 seconds.

The BB filter, a yellow filter with relatively sharp wavelength cut-off, requires only a modest first-order transform to the standard Sloan r' passband. In our hands, using this filter rather than a clear filter or no filter improves night-to-night reproducibility to a degree outweighing loss of signal-to-noise ratio from loss of flux.

FITS images were plate-solved by *PinPoint* (DC-3 Dreams) or *TheSkyX* (Software Bisque) and were calibrated using temperature-matched, median-averaged dark images and recent flat images of a flux-adjustable flat panel. Every photometric image was visually inspected; the author excluded images with poor tracking, obvious interference by cloud or moon, or having stars, satellite tracks, cosmic ray artifacts, or other apparent light sources within 10 arcseconds of the target asteroid. Images passing these screens were submitted to the workflow.

Comparison stars from the ATLAS refcat2 catalog were selected if they had: distance from image boundaries and other catalogued flux sources of at least 15 arcseconds, no catalog VARIABLE flag, Sloan r' magnitude within [-1, +2] of the target asteroid's r' magnitude on that night (except that very faint asteroids used comp stars with magnitudes in the range 14 to 16), Sloan r'-i' color value in the range 0.10 to 0.34, and absence of variability as seen in session plots of each comp star's instrumental magnitude vs time.

In this work, "period" refers to an asteroid's synodic rotation period, "SR" denotes the Sloan r' passband, and "mmag" denotes millimagnitudes (0.001 magnitude).

478 Tergeste. We confirm most known reports of synodic rotational period (15 h, Harris and Young, 1989; 16.104 h, Behrend, 2005web; 16.105 h, Marciniak et al., 2015; 16.107 h, Aznar Macías, 2017; 16.101 h, Brines et al., 2017; several reports near 16.104 h, Marciniak et al., 2018; 16.1011 h, Pál et al., 2020; 16.1 h, Behrend, 2021web) with our estimate of 16.114 ± 0.003 h for this bright outer main-belt asteroid. The lightcurve shape is clearly bimodal, so that our period estimate very probably represents this asteroid's true rotation period. Our Fourier fit RMS error is 4 mmag; best G (H-G model) estimate is 0.15, equal to the MPC nominal G value.

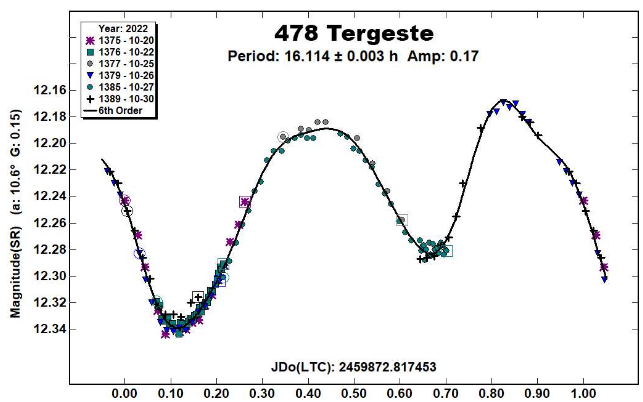

960 Birgit. For this inner main-belt asteroid, we find a rotational period of 8.681 ± 0.002 h, confirming two previous reports (8.85 h, Kryszczyńska et al., 2012; 8.67648 h, Ďurech et al., 2020) but differing from a third (17.3558 h, Behrend, 2005web). The lightcurve shape is unusual enough that this asteroid may represent a shape-modeling opportunity. Our Fourier fit RMS error is 12 mmag.

Number	Name	yyyy mm/dd	Phase	L_{PAB}	B_{PAB}	Period(h)	P.E.	Amp	A.E.	Grp
478	Tergeste	2022 10/20-10/30	10.8,7.2	53	1	16.114	0.003	0.17	0.02	MB-O
960	Birgit	2022 11/07-11/22	26.7,29.0	2	3	8.681	0.002	0.24	0.03	MB-I
1543	Bourgeois	2022 07/09-10/13	*20.1,27.9	324	10	90.768	0.018	0.23	0.04	MB-M
1690	Mayrhofer	2022 10/20-11/24	*8.9,6.0	47	1	19.026	0.002	0.28	0.03	MB-O
1780	Kippes	2022 10/25-12/22	*10.9,10.2	61	8	13.684	0.001	0.09	0.04	EOS
1946	Walraven	2022 12/01-12/27	16.3,6.3	97	10	10.210	0.001	0.88	0.04	MB-I
2085	Henan	2022 09/17-10/22	*11.5,5.4	18	-5	216.890	0.360	0.43	0.08	HEN
3166	Klondike	2022-2023 11/05-01/14	*12.5,20.0	68	0	226.140	0.110	0.77	0.07	MB-I
3229	Solnhofen	2022 10/30-12/01	8.0,17.5	38	12	15.332	0.001	0.43	0.04	MB-I
3560	Chenqian	2022 09/05-10/21	*5.8,13.7	355	6	18.859	0.007	0.05	0.03	EOS
10044	Squyres	2022 10/04-10/26	16.8,20.2	15	20	1.668	0.001	0.10	0.05	MB-I
12746	Yumeginga	2022-2023 11/02-01/05	7.1,27.8	38	4	1239.130	2.240	1.33	0.12	FLO

Table I. Observing circumstances and results. The phase angle is given for the first and last date. If preceded by an asterisk, the phase angle reached an extrema during the period. L_{PAB} and B_{PAB} are the approximate phase angle bisector longitude/latitude at mid-date range (see Harris et al., 1984a). Grp is the asteroid family/group (Warner et al., 2009).

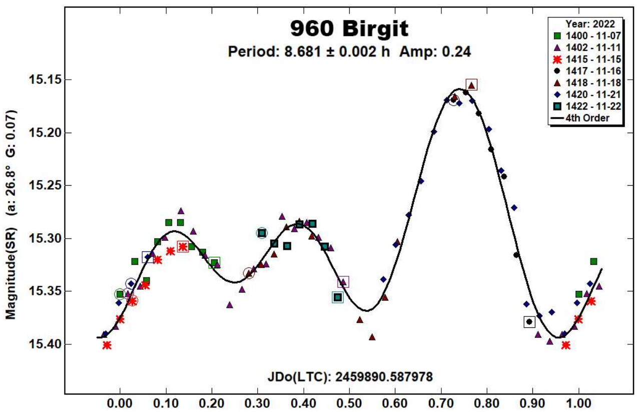

Despite our lightcurve's having only one dominant brightness maximum as well as an amplitude suitable to either a monomodal or bimodal lightcurve interpretation, the period spectrum strongly supports a monomodal (or trimodel if counting all maxima) interpretation with our period estimate as given.

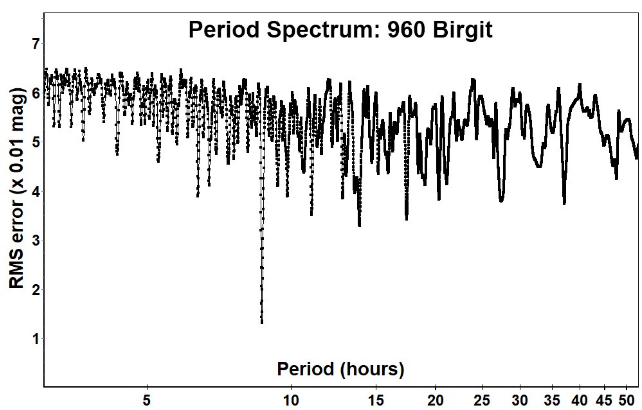

1543 Bourgeois. Our rotational period estimate for this middle main-belt asteroid is 90.768 ± 0.018 h, at wide variance from the sole known report of 2.48 h (Behrend, 2005web), for which the amplitude was reported to be at most 0.03 magnitudes. Several nights of our observations show some evidence of systematic deviation from the best single-period Fourier curve to perhaps 0.02-0.03 magnitudes, which suggests a moderate effect of precession ("tumbling"). Our RMS error is 13 mmag; the best G value is 0.22.

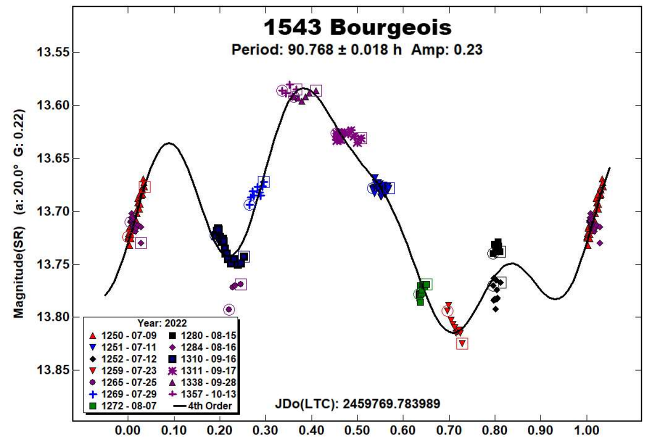

The period spectrum supports our proposed rotational period, though with a noisy character that often accompanies period spectra of processing asteroids. The period spectrum disfavors the previously reported period of 2.48 hours.

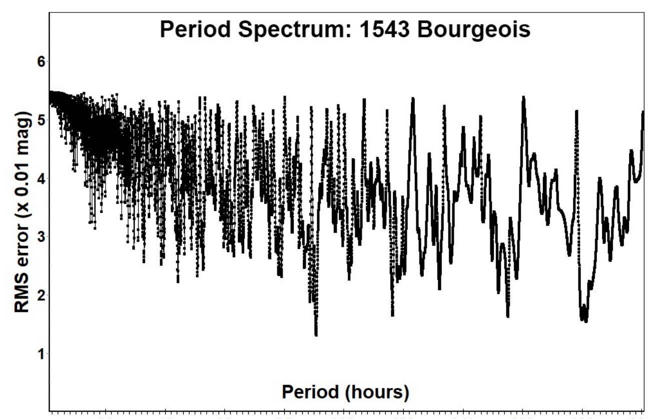

1690 Mayrhofer. For this outer main-belt asteroid during its very favorable 2022 apparition, we find a rotational period of 19.026 ± 0.002 h, agreeing closely with one previous report (19.081 h, Waszczak et al., 2015) and less closely with another (19.5375 h, Pál et al., 2020) but differing from a third (22.194 h, Behrend, 2006web). The lightcurve appears bimodal. Our Fourier fit RMS error is 11 mmag and the best G value was indistinguishable from the MPC nominal value of 0.15.

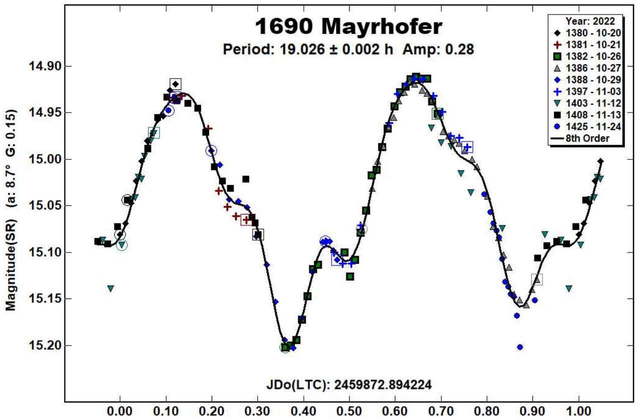

The period spectrum supports our proposed period but offers no support for possible periods near 22-23 h. We can also find no credible alias to associate our proposed period with a period of 22.194 h.

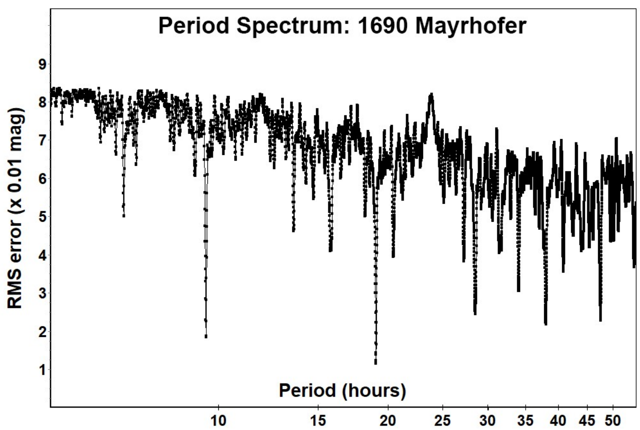

1780 Kippes. Our bimodal period estimate of 13.684 ± 0.01 h differs from both previous reports (18.0 h, Binzel, 1987; 6.83899 h, Pál et al., 2020) for this Eos-family asteroid. The 6.83899 h period candidate is close to one-half of our proposed bimodal period, and is plausible as a monomodal interpretation given the modest amplitude (Harris et al., 2014). We cannot reconcile an 18-hour period with our data, either by fractional multiples or by aliasing. Our RMS error is 15 mmag, and our best G value is very close to MPC's nominal value of 0.15.

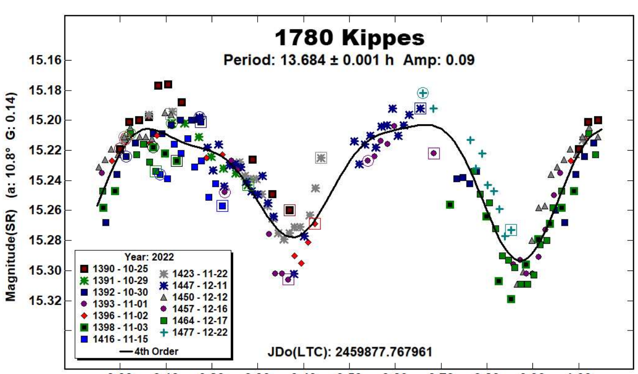

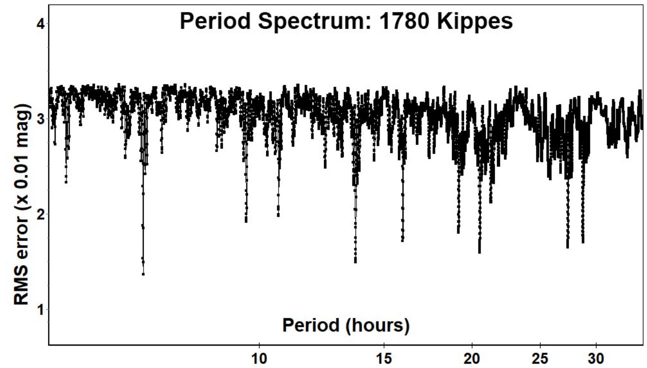

A split-halves phased plot of our data suggests but does not compel a bimodal interpretation in preference to monomodality.

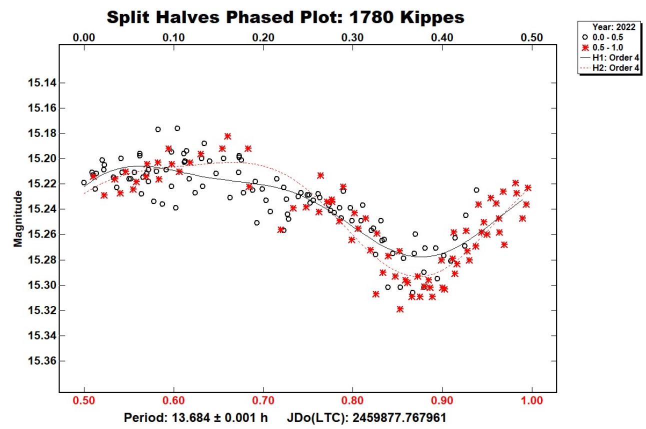

1946 Walraven. Our lightcurve for this high-amplitude inner main-belt asteroid matches all known reports (10.233 h, van Gent, 1933; 10.22 h, Folberth et al., 2012; 10.21 h, Aznar Macías et al., 2016; 10.2101 h, Hanuš et al., 2016; 10.1881 h, Pál et al., 2020). For our proposed period of 10.2095 ± 0.0005 h, our RMS error is 21 mmag, and our best G value estimate is 0.45.

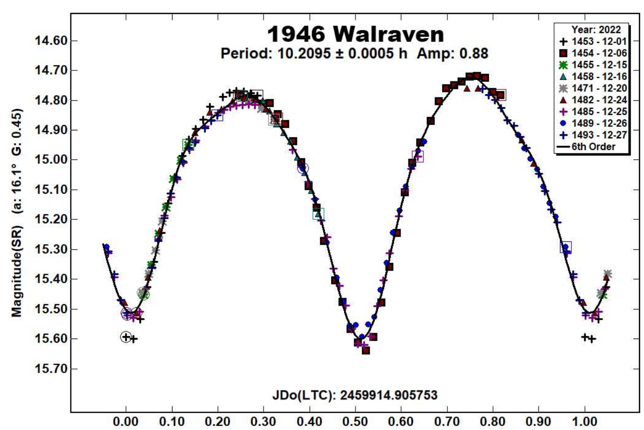

The period spectrum shows major signals only at multiples of ½ our proposed period. Of these, the deepest signal and high amplitude strongly recommend a bimodal interpretation.

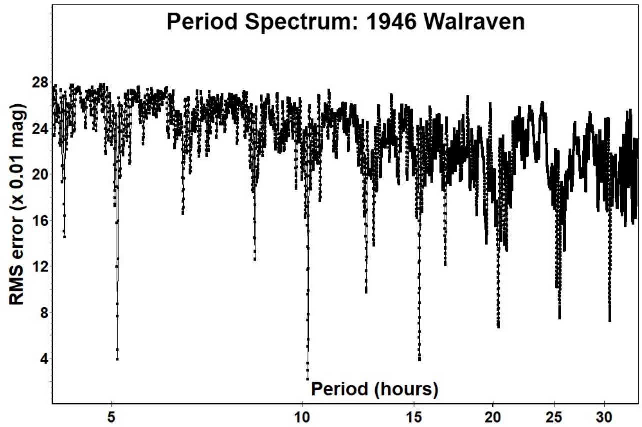

2085 Henan. This asteroid, the parent body of the Henan family, has three period reports (110 h, Devogèle et al., 2017; 221.71 h, Ďurech et al., 2020; 221.709550 h, Martikainen et al., 2021), as well as one reported constraint (> 24 h, Behrend, 2004web) which the LCDB currently gives as the best current period estimate. We find a period of 216.89 ± 0.36 h from 14 nights of data over 5 weeks (3.9 period cycles). Systematic deviations from a smooth lightcurve suggest precession ("tumbling") for this long-period asteroid. Our Fourier fit RMS error is 34 mmag; our best G estimate is 0.19, but that estimate does not give a clearly superior fit relative to the MPC nominal value of 0.15.

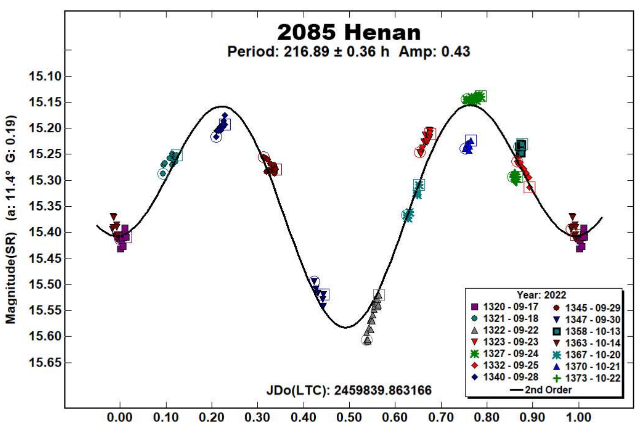

The relatively high amplitude of 0.43 magnitudes, the lightcurve shape, and the period spectrum's single major feature all suggest a bimodal interpretation with period near 220 h, disfavoring a monomodal interpretation that would yield a period near 110 h.

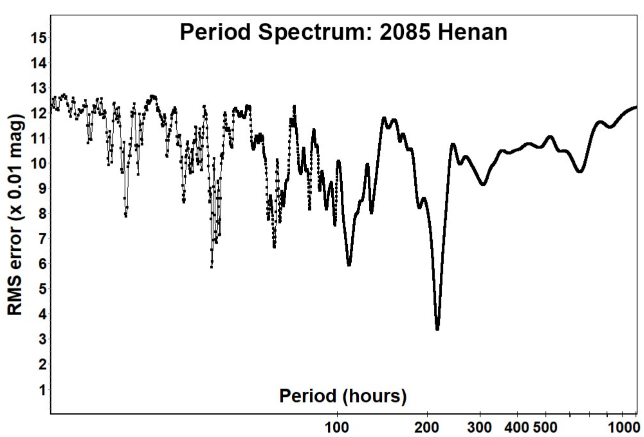

3166 Klondike. For this inner main-belt asteroid, we find a rotational period of 226.14 h, consistent with two reported lower limits (>20 h, Behrend, 2007web; >20h, Pravec et al., 2007web) but differing from all known period estimate reports (11.72 h, Sauppe et al., 2007; 150.707 h, Ďurech et al., 2020; 75.288 h, Pál et al., 2020; 150.19 h, Ferrero, 2020; 157.7 h, Polakis, 2020). Our Fourier fit RMS error is 30 mmag; fits with our G estimate of 0.27 were much better than those with MPC's nominal value of 0.15.

The lightcurve has a remarkable shape, being essentially trimodal, and it shows little or no effect of any precession ("tumbling"). Lightcurve and period determination were aided not only by the large amplitude, but by the short feature durations, which resulted in sizeable brightness changes, even within several of the shorter observing sessions.

The trimodal shape persisted through our observing campaign of almost 8 rotations, and it is likely the cause of our estimate's being 1.5 times the estimate of several recent reports.

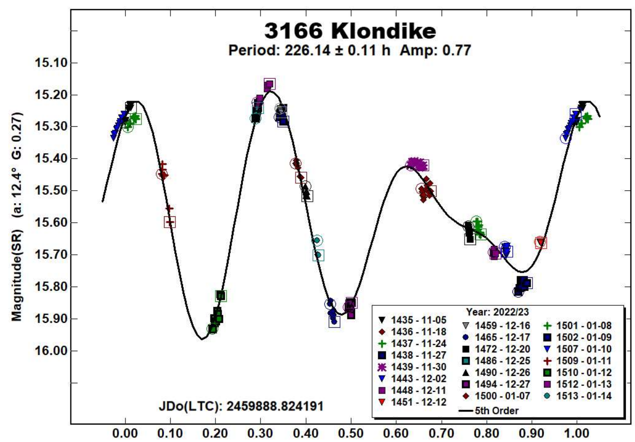

Our period spectrum does not support previously reported periods around 75 or 150 hours (one-third and two-thirds of our period estimate), though those do appear as minor spectral features.

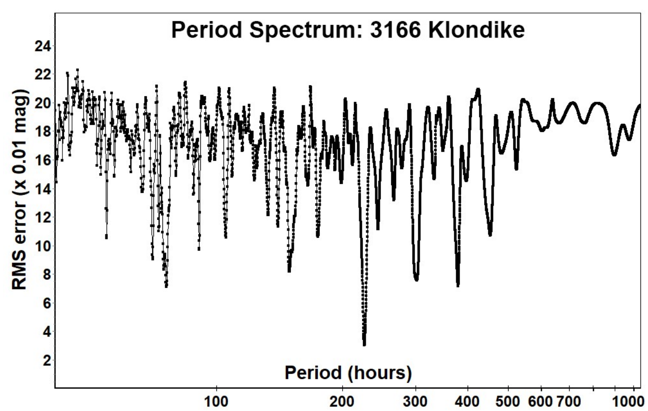

3229 Solnhofen. Our synodic rotational period estimate of 15.332 ± 0.01 h for this inner main-belt asteroid differs from the sole known previous report (11.52 h, Folberth et al., 2012), which is an alias of our result by ½ period per 24 hours. Our Fourier fit RMS error is 16 mmag; our best G value estimate of 0.32 gives much lower fit RMS errors than do fits using MPC's nominal value of 0.15.

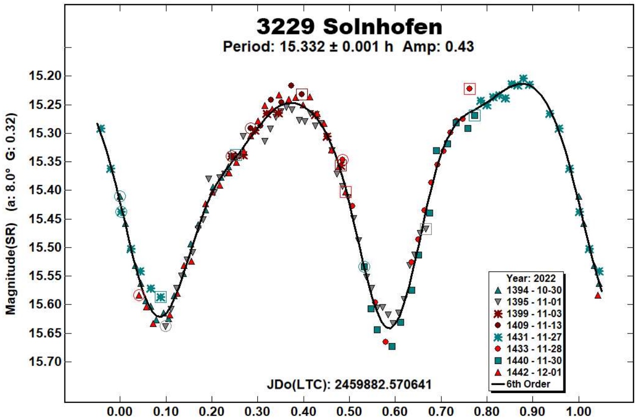

Major signals in our period spectrum appear only at multiples of half our proposed period. The lightcurve shape (especially shape around the maxima), the strongest period spectrum signal, and the relatively high amplitude all support the bimodal interpretation adopted here. The previously reported period of 11.52 h does not appear as major signal in this period spectrum.

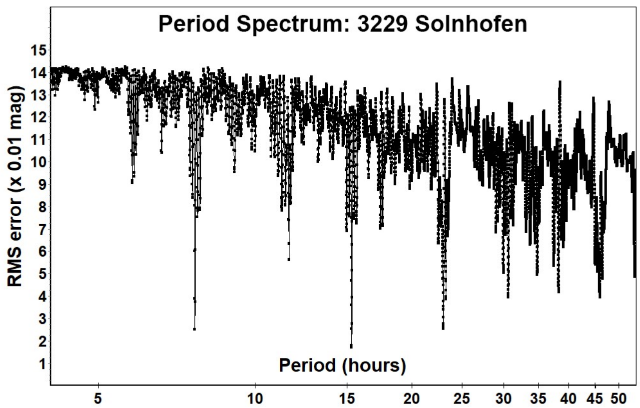

3560 Chenqian. This Eos-family asteroid's 2022 apparition gave a much smaller rotational amplitude (0.05 magnitudes) than previously reported in the LCDB (0.17-0.26). Despite this, we estimate a monomodal-basis rotational period of 18.859 ± 0.007 h, agreeing well with two previous reports (18.79 h, Pligge et al., 2011; 18.8003 h, Ďurech et al., 2020) but disagreeing with one other (12.454 h, Behrend, 2019web). Our RMS error is 10 mmag, using our best G estimate of 0.03.

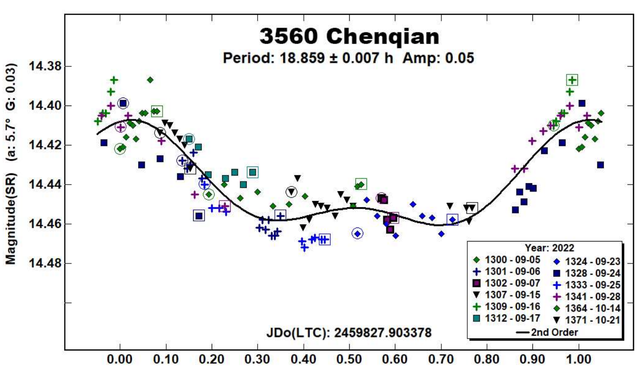

The period spectrum shows no signal at the previously reported period of 12.454 h.

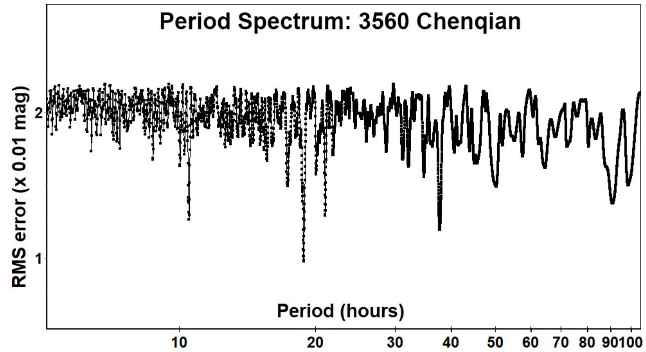

10044 Squyres. No rotational period reports are known for this inner main-belt asteroid. We offer a period estimate of 1.668 ± 0.001 h on a monodal basis from our low signal-to-noise photometric data. Fourier fit RMS error is 25 mmag, about half the measured amplitude. The best G value estimate of 0.45 is of very low confidence, as the exact value made little difference to fit quality.

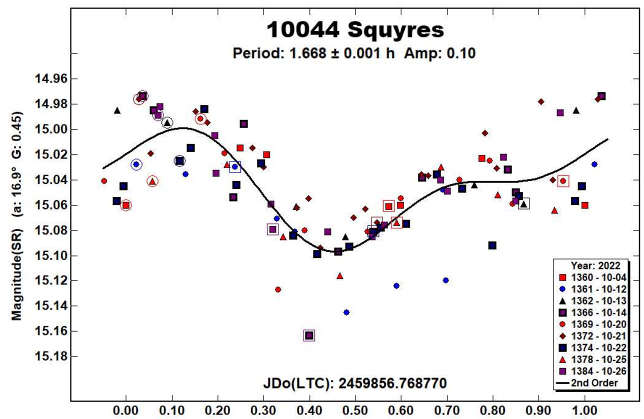

Choosing between monomodal (P=1.668 h) and bimodal (3.336 h) interpretations is not helped by the lightcurve shape, the lightcurve amplitude, or the period spectrum. We report a monomodal period, but a bimodal period is also quite consistent with our data. The current data do appear to rule out periods longer than 3.4 hours. July 2026 offers an especially favorable apparition, visible to both North and South hemispheres, and observations with larger amateur telescopes are encouraged.

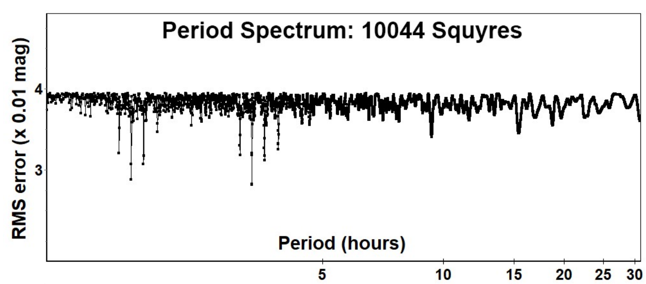

12746 Yumeginga. No previous rotational period reports are known for this Flora asteroid. We report an extraordinary period of 1239.13 ± 2.24 h (bimodal basis) from 25 nights' observations over 10 weeks. The lightcurve displays an exceptional amplitude of 1.33 magnitudes and so is assigned a bimodal interpretation even though the phased lightcurve's halves are similar. We saw no effect of precession ("tumbling"). Fourier fit RMS error is 47 mmag; best G estimate is 0.18.

Our campaign began just after maximum brightness and continued until the asteroid became too faint for the author's equipment (asteroid signal-to-noise ca. 30); despite the campaign's length, it covered only 1.34 rotations, being almost 3 max-min cycles.

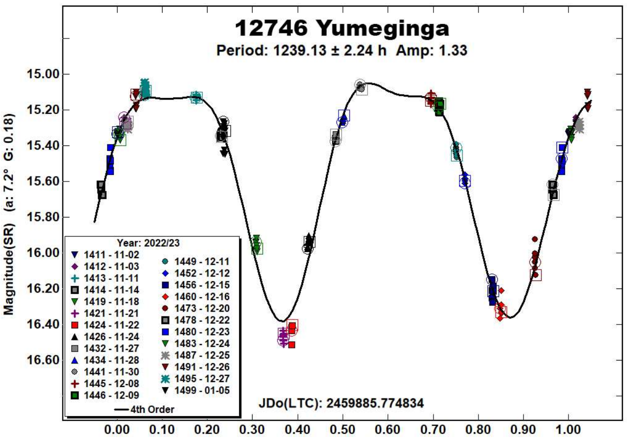

Because this observing campaign was only slightly longer than the proposed period, even longer periods can be only weakly ruled out by the period spectrum itself. However, it hard to imagine any longer period's giving a better bimodal fit to our observation data than that depicted in the phased lightcurve plot above.

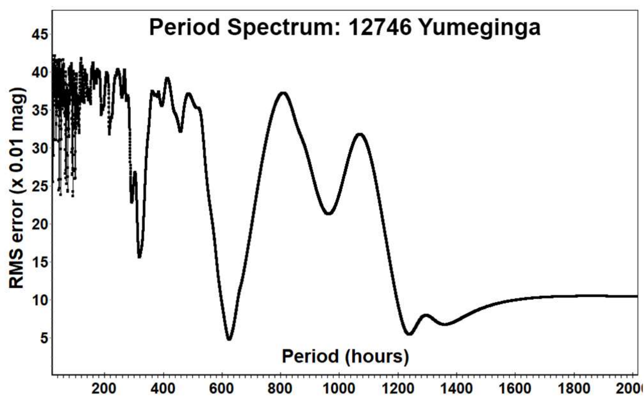

The next favorable apparition in July 2025, with declination -17°, might seem to favor the Southern over the Northern hemisphere, but sky elevation will matter much less for this apparition than for most. That is, given this asteroid's very long period, reliable 4-hour sessions in the Northern Hemisphere will be practically as useful as 9-hour sessions in the Southern. More important than long sessions will be the number of nights observed and length of observing campaigns in months. Getting an early start will be essential.

Acknowledgements

The author thanks all the authors of and contributors to the ATLAS paper (Tonry et al, 2018) for providing openly and without cost the ATLAS refcat2 catalog release. This current work also makes extensive use of the python language interpreter and of several supporting packages (notably: astropy, ccdproc, ephem, matplotlib, pandas, photutils, requests, and statsmodels), all made available openly and without cost.

References

Aznar Macías, A.; Garcerán, A.C.; Mansego, E.A.; Rodriguez, P.B.; Lozano, J.d.H.; Silva, A.F.; Silva, F.S.; Martinez, V.M.; Chiner, O.R.; Porta, D.H. (2016). "Twenty-one Asteroid Lightcurves at Group Observadores de Asteroides (OBAS): Late 2015 to Early 2016." *Minor Planet Bull*. **43**, 257-263.

Aznar Macías, A. (2017). "Lightcurve Analysis for Nine Main-belt Asteroids. Rotation Period and Physical Parameters from APT Observatory Group: 2016 October - December." *Minor Planet Bull*. **44**, 139-141.

Behrend, R. (2004web, 2005web, 2006web, 2007web, 2019web, 2021web). Observatoire de Genève web site. *http://obswww.unige.ch/~behrend/page_cou.html*

Binzel, R.P. (1987). "A photoelectric survey of 130 asteroids." *Icarus* **72**, 135-208.

Brines, P.; Lozano, J.; Rodrigo, O.; Fornas, A.; Herrero, D.; Mas, V.; Fornas, G.; Carreño, A.; Arce, E. (2017). "Sixteen Asteroids Lightcurves at Asteroids Observers (OBAS) - MPPD: 2016 June - November." *Minor Planet Bull*. **44**, 145-149.

Devogèle, M. and 53 colleagues (2017). "Shape and spin determination of Barbarian asteroids." *Astron. Astrophys.* **607**, A119.

Dose, E. (2020). "A New Photometric Workflow and Lightcurves of Fifteen Asteroids." *Minor Planet Bull*. **47**, 324-330.

Dose, E. (2021). "Lightcurves of Nineteen Asteroids." *Minor Planet Bull*. **48**, 69-76.

Ďurech, J.; Tonry, J.; Erasmus, N.; Denneau, L.; Heinze, A.N.; Flewelling, H.; Vančo, R. (2020). "Asteroid models reconstructed from ATLAS photometry." *Astron. Astrophys.* **643**, A59.

Ferrero, A. (2020). "Photometric Lightcurves of Eight Main-Belt Asteroids." *Minor Planet Bull*. **47**, 172-174.

Folberth, J.; Casimir, S.; Dou, Y.; Evans, D.; Foulkes, T.; Haenftling, M.; Kuhn, P.; White, A.; Ditteon, R. (2012). "Asteroid Lightcurve Analysis at the Oakley Southern Sky Observatory: 2011 July - September." *Minor Planet Bull*. **39**, 51-55.

Hanuš, J. and 168 colleagues (2016). "New and updated convex shape models of asteroids based on optical data from a large collaboration network." *Astron. Astrophys.* **586**, A108.

Harris, A.W.; Young, J.W.; Scaltriti, F.; Zappalà, V. (1984a). "Lightcurves and phase relations of the asteroids 82 Alkmene and 444 Gyptis." *Icarus* **57**, 251-258.

Harris, A.W. and 15 colleagues (1984b). "On the maximum amplitude of harmonics of an asteroid lightcurve." *Icarus* **235**, 55-59.

Harris, A.W.; Young, J.W. (1989). "Asteroid lightcurve observations from 1979-1981." *Icarus* **81**, 314-364.

Harris, A.W.; Pravec, P.; Galad, A.; Skiff, B.A.; Warner, B.D.; Vilagi, J.; Gajdos, S.; Carbognani, A.; Hornoch, K.; Kusnirak, P.; Cooney, W.R.; Gross, J.; Terrell, D.; Higgins, D.; Bowell, E.; Koehn, B.W. (2014). "On the maximum amplitude of harmonics on an asteroid lightcurve." *Icarus* **235**, 55-59.

Kryszczyńska, A. and 29 colleagues (2012). “Do Slivan states exist in the Flora family? I. Photometric survey of the Flora region.” *Astron. Astrophys.* **546**, A72.

Marciniak, A. and 23 colleagues (2015). “Against the biases in spins and shapes of asteroids.” *Planetary Space Sci.* **118**, 256-266.

Marciniak, A. and 42 colleagues (2018). “Photometric survey, modelling, and scaling of long-period and low-amplitude asteroids.” *Astron. Astrophys.* **610**, A7.

Martikainen, J.; Muinonen, K.; Penttilä, A.; Cellino, A.; Wang, X.-B. (2021). “Asteroid absolute magnitudes and phase curve parameters from *Gaia* photometry.” *Astron. Astrophys.* **649**, A98.

Pál, A.; Szakáts, R.; Kiss, C.; Bódi, A.; Bognár, Z.; Kalup, C.; Kiss, L.L.; Marton, G.; Molnár, L.; Plachy, E.; Sárneczky, K.; Szabó, G.M.; Szabó, R. (2020). “Solar System Objects Observed with TESS - First Data Release: Bright Main-belt and Trojan Asteroids from the Southern Survey.” *Ap. J.* **247**, A26.

Pligge, Z.; Monnier, A.; Pharo, J.; Stolze, K.; Yim, A.; Ditteon, R. (2011). “Asteroid Lightcurve Analysis at the Oakley Southern Sky Observatory: 2010 May.” *Minor Planet Bull*. **38**, 5-7.

Polakis, T. (2020). “Photometric Observations of Thirty Minor Planets.” *Minor Planet Bull*. **47**, 177-184.

Pravec, P.; Wolf, M.; Sarounova, L. (2007web). Ondrejov Asteroid Photometry Project. *https://www.asu.cas.cz/~ppravec/neo.htm*

Sauppe, J.; Torno, S.; Lemke-Oliver, R.; Ditteon, R. (2007). “Asteroid Lightcurve Analysis at the Oakley Observatory – March/April 2007.” *Minor Planet Bull*. **34**, 119-122.

Tonry, J.L.; Denneau, L.; Flewelling, H.; Heinze, A.N.; Onken, C.A.; Smartt, S.J.; Stalder, B.; Weiland, H.J.; Wolf, C. (2018). “The ATLAS All-Sky Stellar Reference Catalog.” *Astrophys. J.* **867**, A105.

van Gent, H. (1933). “Period, lightcurve and ephemeris of the new asteroid with variable brightness 1931 PH.” *Bull. Astron. Institutes Netherlands* **7**, 65-66.

Warner, B.D.; Harris, A.W.; Pravec, P. (2009). “The asteroid lightcurve database.” *Icarus* **202**, 134-146. *https://minplanobs.org/MPInfo/php/lcdb.php*

Warner, B.D. (2021). *MPO Canopus* Software, version 10.8.4.11. BDW Publishing. *http://www.bdwpublishing.com*

Waszczak, A.; Chang, C.-K.; Ofek, E.O.; Laher, R.; Masci, F.; Levitan, D.; Surace, J.; Cheng, Y.-C.; Ip, W.-H.; Kinoshita, D.; Helou, G.; Prince, T.A.; Kulkarni, S. (2015). “Asteroid Light Curves from the Palomar Transient Factory Survey: Rotation Periods and Phase Functions from Sparse Photometry.” *Astron. J.* **150**, A75.

MAIN-BELT AND TROJAN ASTEROIDS OBSERVED FROM CS3: 2022 OCTOBER-NOVEMBER

Robert D. Stephens
Center for Solar System Studies (CS3)
11355 Mount Johnson Ct., Rancho Cucamonga, CA 91737 USA
rstephens@foxandstephens.com

(Received: 2022 December 16)

CCD photometric observations of three main-belt asteroids and four Jovian Trojans from the L4 cloud were obtained at the Center for Solar System Studies (CS3) from 2022 October-November. Revised periods for 4060 Deipylos from previous oppositions are also reported.

The Center for Solar System Studies (CS3) has nine telescopes which are normally used in program asteroid family studies. The focus is on near-Earth asteroids, Jovian Trojans and Hildas. When it is not the season to study a family, or when a nearly full moon is too close to the family targets being studied, targets of opportunity amongst the main-belt families were selected.

Table I lists the telescopes and CCD cameras that were used to make the observations. Images were unbinned with no filter and had master flats and darks applied. The exposures depended upon various factors including magnitude of the target, sky motion, and Moon illumination.

Telescope	Camera
0.40-m f/10 Schmidt-Cass	FLI Proline 1001E
0.50-m F/8.1 R-C	FLI Proline 1001E

Table I: List of CS3 telescope/CCD camera.

Image processing, measurement, and period analysis were done using *MPO Canopus* (Bdw Publishing), which incorporates the Fourier analysis algorithm (FALC) developed by Harris (Harris et al., 1989). The Comp Star Selector feature in *MPO Canopus* was used to limit the comparison stars to near solar color. Night-to-night calibration was done using field stars from the ATLAS catalog (Tonry et al., 2018), which has Sloan *griz* magnitudes that were derived from the GAIA and Pan-STARR catalogs and are “native” magnitudes of the catalog. Those adjustments are usually ≤ ±0.03 mag. The rare greater corrections may have been related in part to using unfiltered observations, poor centroiding of the reference stars, and not correcting for second-order extinction.

The Y-axis values are ATLAS SR “sky” magnitudes. The two values in the parentheses are the phase angle (a) and the value of *G* used to normalize the data to the comparison stars used in the earliest session. This, in effect, made all the observations seem to be made at a single fixed date/time and phase angle, leaving any variations due only to the asteroid’s rotation and/or albedo changes. The X-axis shows rotational phase from -0.05 to 1.05. If the plot includes the amplitude, e.g., “Amp: 0.65”, this is the amplitude of the Fourier model curve and *not necessarily the adopted amplitude for the lightcurve*.

For brevity, only some of the previously reported rotational periods may be referenced. A complete list is available at the asteroid lightcurve database (LCDB; Warner et al., 2009).